

High Power Three-Section Integrated Master Oscillator Power Amplifier at $1.5\ \mu\text{m}$

Mickaël Faugeron, Mariafernanda Vilera, Michel Krakowski, Yannick Robert, Eric Vinet, Peppino Primiani, Jean-Pierre Le Goëc, Olivier Parillaud, Antonio Pérez-Serrano, Jose Manuel G. Tijero, Gerd Kochem, Martin Traub, Ignacio Esquivias, and Frédéric van Dijk

Abstract—We present the design and the performance of a monolithically integrated master oscillator power amplifier at $1.5\ \mu\text{m}$. The three-section device includes a distributed feedback laser, a modulation section, and a high power tapered amplifier. In order to mitigate the coupling effects of the light reflected at the facets, the device has been designed with a bent longitudinal axis and a tilted front facet. The device delivers $>400\ \text{mW}$ mode-hopping free output power. In static regime, the modulation section allows an extinction ratio of 35 dB.

Index Terms—Distributed feedback lasers, semiconductor optical amplifier, integrated optics devices, multi-section laser, master oscillator power amplifier.

I. INTRODUCTION

AN INCREASING number of applications such as free-space communications, lidar systems, telemetry or spectroscopy require high power single-mode lasers around $1.55\ \mu\text{m}$. Nowadays the most used sources for these applications are solid-state lasers and fiber lasers. In this field semiconductor devices have still to demonstrate high power operation ($>0.5\ \text{W}$) in order to be credible competitors. Indeed semiconductor devices have lots of advantages in terms of weight and compactness or wall-plug efficiency. In addition they have also demonstrated high radiation hardness, being thus promising sources for space-borne applications.

The maximum output power obtained from distributed feedback (DFB) lasers and semiconductor external cavity

lasers is below $0.45\ \text{W}$ [1], [2]. The Master Oscillator Power Amplifier (MOPA) seems the most promising configuration to reach both high power and single-mode operation. A MOPA usually consists of two sections, a distributed Bragg reflector (DBR) or DFB laser acting as a master oscillator and a power amplifier. Thanks to the progresses made in the fabrication processes, it is possible to integrate on the same chip both master oscillator and power amplifier, as well as additional sections allowing various complex functionalities (modulation, pre-amplification, photodetection, etc...). Unlike hybrid counterparts, the integration on the same chip simplifies the complexity of the packaging and reduces its cost. At $1.55\ \mu\text{m}$, output power up to $1.5\ \text{W}$ under continuous wave (CW) operation has already been demonstrated with a monolithically integrated commercial two-section straight MOPA [3].

In a MOPA working at ideal conditions, the single-mode generated by the master oscillator is amplified by the amplifier section keeping its initial beam quality. In practical devices, the most important challenge is to reduce the reflections, mainly at the flared SOA facet. Indeed, even with good anti-reflection (AR) coatings, the residual reflections can disturb the DFB behavior and enhance coupled cavities effects, leading to multimode operation and mode hopping. Several works have highlighted these phenomena on straight MOPAs [4], [5]. For system applications, it implies to choose a precise set of parameters (temperature and bias current on the different sections) in order to have a single-mode emission. Recently, Hou et al. have demonstrated single-mode operation by curving the flared amplifier obtaining an output power of $0.2\ \text{W}$ [6].

In this letter, we present the design and performance of a three-section bent MOPA. The first section is a DFB laser acting as the master oscillator; the third section is a flared semiconductor optical amplifier (SOA) to boost the optical signal. Between these 2 sections, a curved modulation section is implemented in order to allow the modulation of the light coming from the DFB laser while favoring single-mode operation. Among the numerous possible applications of implementing a modulation section in such devices, the presented devices are intended to be used in Random Modulated Continuous Wave (RM-CW) Integrated Path Differential Absorption (IPDA) lidar systems [7].

The letter is organized as follows. The design and fabrication of the MOPAs are described in Section II and Section III respectively. In Section IV, the experimental results

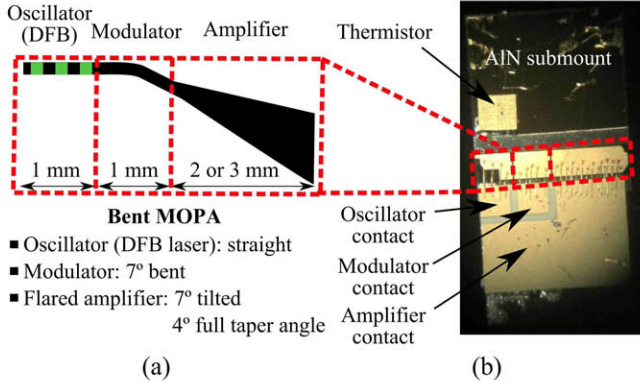


Fig. 1. (a) Schematics of a bent MOPA. (b) Mounted device.

on the characterization of the devices are shown; including the power-current characteristic, optical spectra, extinction ratio induced by current variations on the modulation section in static regime, and the beam characteristics by means of far and near field measurements. Finally, the conclusions are summarized in Section V.

II. DESIGN OF THE MOPA STRUCTURE

The epitaxial design is based on an asymmetrical cladding structure which has previously demonstrated very good performances for DFB and Fabry-Perot (FP) lasers [8], [9]. This method allows decreasing drastically the internal losses due to the low overlap of the enlarged optical mode with the p-doped layers. The dilute waveguide was composed of 14 periods of InGaAsP ($\lambda_g = 1.17 \mu\text{m}$)/InP layers. The total waveguide was $1.53 \mu\text{m}$ thick. More details about the principle of dilute waveguide are given in [10].

Fig. 1(a) shows the schematics of the three-section high power MOPA. The first section is a 1 mm long DFB laser, acting as the master oscillator, with a $3 \mu\text{m}$ wide Ridge Waveguide (RW) structure and grating strength (κL) of around 1.3. The second section is also a $3 \mu\text{m}$ wide RW which acts as modulator by absorbing or amplifying the DFB emission when it is driven at zero or forward voltage. The third section is a flared semiconductor optical amplifier (SOA) with a length $L_{SOA} = 2$ or 3 mm and a full taper angle of 4° . The amplifier waveguide width at the output facet is $147 \mu\text{m}$ (2 mm long SOA) and $218 \mu\text{m}$ (3 mm long SOA).

In order to avoid laser action in SOAs, it is a common practice to tilt the RW to decrease the coupling of the reflection at the facets into the cavity mode [11]. In the case of DFB based MOPAs, a tilted DFB section would difficult the precise control of the reflectivity at the back facet coating. To solve this problem in a two-section MOPA, Hou et al. have introduced a bend at the beginning of the flared SOA [6]. We have implemented a bent modulation section which gives rise to a 7° tilt of the flared SOA longitudinal axis with respect to the front facet. Simulations of the bend losses with BeamPROP [12] indicated that a 0.7 mm long modulator section (5.7 mm radius of curvature) was necessary to achieve propagation losses lower than 1 dB. The length of the

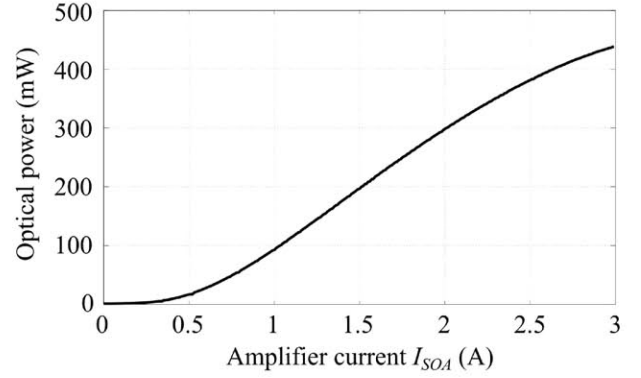


Fig. 2. P-I measurement for $I_{DFB} = 400 \text{ mA}$ and $I_{mod} = 300 \text{ mA}$ while varying I_{SOA} . $L_{SOA} = 2 \text{ mm}$.

modulation section was set to 1 mm to ensure this low value of the propagation losses.

III. FABRICATION

The epitaxial structure was grown by Metal Organic Vapor Phase Epitaxy (MOVPE) on n-type InP substrates. It includes six 8 nm thick compressively strained (0.85%) InGaAsP quantum wells and five 10 nm thick InGaAsP ($\lambda_g = 1.17 \mu\text{m}$) barriers. The measured photoluminescence peak was $1.57 \mu\text{m}$. For the electric isolation of the different sections the inter-section regions were defined by removing the metallization and the p-doped contact layer followed by the ionic implantation of the region. We measured an inter-section resistance about $2 \text{ k}\Omega$. A $4 \mu\text{m}$ thick gold layer was deposited onto the surface to improve heat dissipation and to allow electrical bonding with minimum damage.

The devices were high-reflectivity ($HR = 90 \%$) coated on the DFB laser backside facet and anti-reflection ($AR < 10^{-3}$) coated on the SOA facet. The chips were soldered p-side up on aluminum nitride (AlN) submounts using Au-Sn solder pads. An alumina chip with three pads, one for each section, was also soldered onto the AlN submount and connected with the device by ball-bonding. A thermistor was glued onto the submount for an accurate control of the chip temperature. A photograph of a mounted device is shown in Fig. 1 (b).

IV. EXPERIMENTAL RESULTS

Power-current characteristics, optical spectra with a resolution of 0.07 nm and far-field profiles were measured for different devices. All measurements were performed at 18°C .

Fig. 2 shows the output power as function of the flared SOA current ($L_{SOA} = 2 \text{ mm}$). The maximum measured power is about 430 mW for $I_{DFB} = 400 \text{ mA}$, $I_{mod} = 300 \text{ mA}$ and $I_{SOA} = 3 \text{ A}$. The main limitation for the maximum optical power is related to thermal saturation at quite low current density (2 kA cm^{-2}). In a similar device reported in [9], this saturation occurs for a higher current density (4.64 kA cm^{-2}). The thermal saturation is attributed to the series resistance which is four times higher (4Ω for the 1 mm long DFB laser of the MOPA chip) than expected [10] due to a problem during the annealing process of the ohmic contact. By decreasing the

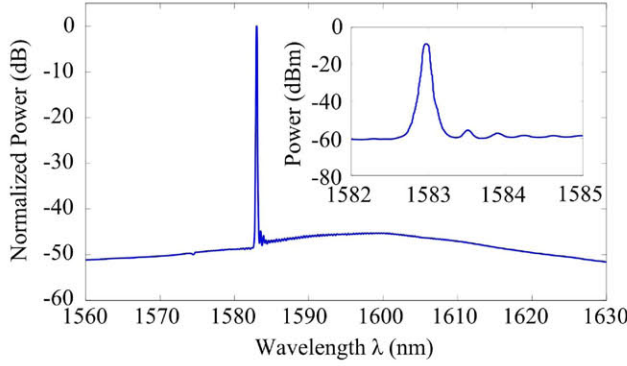


Fig. 3. Optical spectrum for $I_{DFB} = 400$ mA, $I_{mod} = 300$ mA and $I_{SOA} = 3$ A. $L_{SOA} = 2$ mm.

temperature to 12 and 6 °C, the maximum output power was 510 and 600 mW respectively.

A fraction of the total output power was collected using a lensed fiber to record the optical spectra, as shown in Fig. 3 for $I_{DFB} = 400$ mA, $I_{mod} = 300$ mA and $I_{SOA} = 3$ A ($L_{SOA} = 2$ mm). The peak position at around 1583 nm and a side-mode suppression-ratio (SMSR) better than 45 dB are shown in the inset. The single-mode peak is 17 nm blue-shifted compared with the maximum of the amplified spontaneous emission (ASE) spectrum. Some residual spectral peaks can be observed. The separation between them is 43.8 GHz (0.37 nm) which corresponds to a 1 mm long FP equivalent cavity. These FP modes are generated between the back facet of the DFB and the inter-electrode region between the DFB and the modulator.

Fig. 4 shows the evolution of the optical spectra for a device with $L_{SOA} = 3$ mm, as a function of I_{DFB} for $I_{mod} = 300$ mA and $I_{SOA} = 1$ A (a), 2 A (b) and 3 A (c). The wavelength shift (~ 3.2 pm/mA) as a function of I_{DFB} is due to heating effects. At low I_{DFB} , one peak at each side of the stop-band (~ 0.5 nm) is observed due to the absence of a phase shift in the DFB, together with some FP oscillations. Above $I_{DFB} = 250$ mA, the SMSR is higher than 35 dB and single-mode operation without any mode hopping is observed.

In order to quantify the modulation capability, the attenuation introduced by the modulator in static conditions was defined in terms of the extinction ratio, as

$$Att_{dB}(I_{mod}) = 10 \log \left(\frac{P(I_{mod})}{P_{max}} \right) \quad (1)$$

where P_{max} is the optical power for $I_{mod} = 300$ mA. Fig. 5 (a) shows this attenuation as a function of I_{mod} between $I_{mod} = -127$ mA (corresponding to 0 V) and $I_{mod} = 300$ mA. The attenuation goes down from 35 to 0 dB. Approximately at -100 mA the voltage in the modulator section is ≈ 0.7 V; above this value the absorption becomes low and the attenuation is very poor. It is remarkable to notice that under these injection conditions the optical spectrum remains single-mode and very stable for the whole set of I_{mod} as can be observed in Fig. 5 (b). Preliminary modulation response measurements indicate a -3 dB modulation bandwidth between 1 and 2 GHz as a function of the bias currents.

The specific design of the devices has two main effects on the far field. First, the 7° tilting of the SOA front facet makes the output beam to deviate by about 23° in the lateral axis

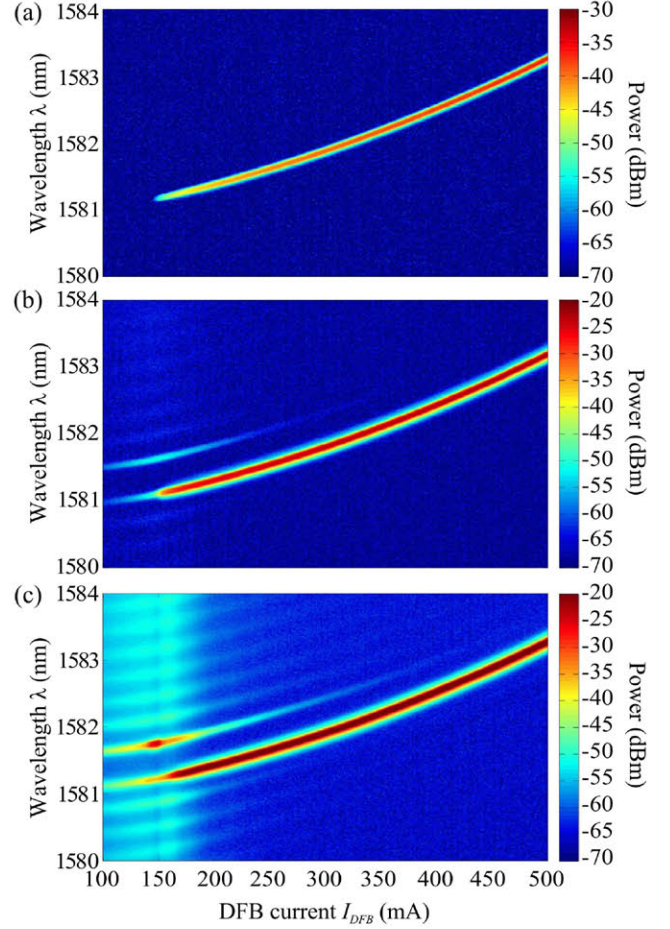


Fig. 4. Optical spectra while varying I_{DFB} for (a) $I_{mod} = 300$ mA and $I_{SOA} = 1$ A, (b) $I_{mod} = 300$ mA and $I_{SOA} = 2$ A, (c) $I_{mod} = 300$ mA and $I_{SOA} = 3$ A. $L_{SOA} = 3$ mm.

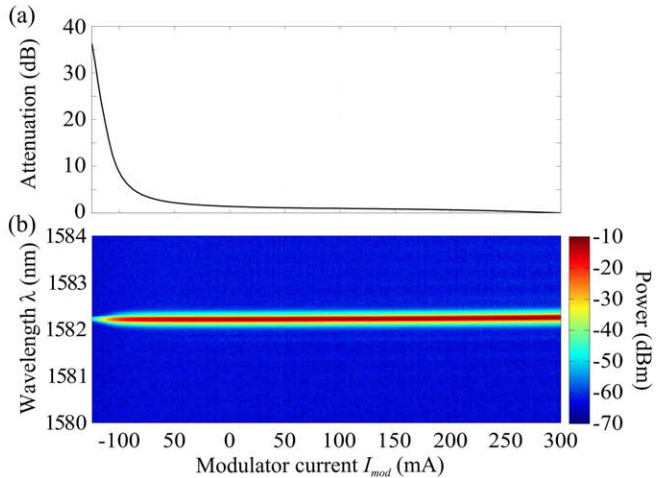


Fig. 5. Impact of the modulator current I_{mod} on the output power. $I_{DFB} = 500$ mA and $I_{SOA} = 3$ A. (a) Attenuation. (b) Optical spectra.

direction. Second, the asymmetric cladding epitaxial structure decreases the far field full width at half maximum (FWHM) in the fast axis to about 23.5° , thus contributing to facilitate the beam shaping and coupling.

Figs. 6 and 7 illustrate the details of the far field. For clarity, the 23° offset has been removed and the far field

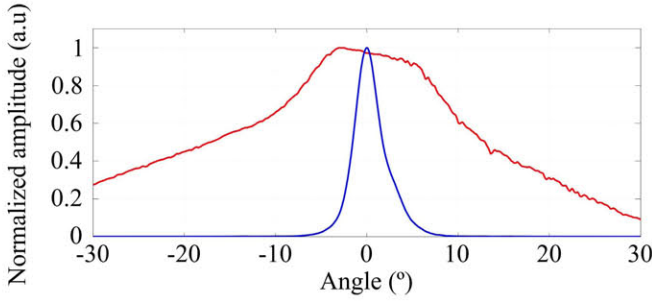


Fig. 6. Impact of the injection in the slow axis far field. Blue line: $I_{DFB} = 250$ mA, $I_{mod} = 150$ mA and $I_{SOA} = 1$ A. Red line: $I_{DFB} = 0$ mA, $I_{mod} = 0$ mA and $I_{SOA} = 1$ A. $L_{SOA} = 3$ mm.

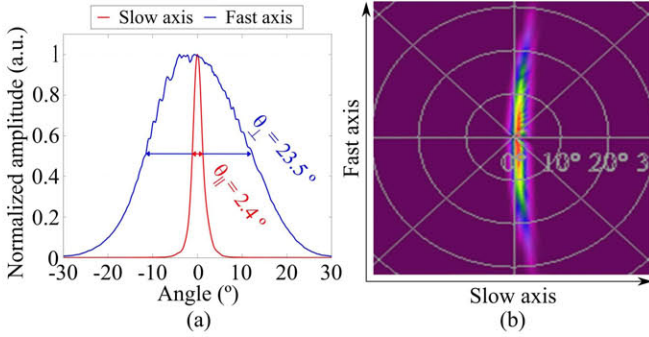


Fig. 7. Far field for $I_{DFB} = 350$ mA, $I_{mod} = 300$ mA and $I_{SOA} = 2$ A. (a) Slow and fast axes far field. (b) 2D far field. $L_{SOA} = 3$ mm.

profiles have been centered at 0° in all the plots. Fig. 6 shows the narrow far field profile in the slow axis recorded when the SOA is electrically biased ($I_{SOA} = 1$ A) and optically injected ($I_{DFB} = 250$ mA, $I_{mod} = 150$ mA). For comparison, the broad far field profile (FWHM $> 20^\circ$) due to spontaneous emission when the SOA is not optically injected has also been plotted. Fig. 7 shows the far field profiles in the slow and fast axis under optical injection ($I_{DFB} = 350$ mA, $I_{mod} = 300$ mA and $I_{SOA} = 2$ A). The FWHM are 2.4° and 23.5° respectively (see Fig. 7(a)). Due to the astigmatism and the tilting of the SOA facet, the far field pattern is crescent-shaped [13], as can be seen in Fig. 7 (b). The slow axis beam quality M^2 was measured using a spherical fast axis collimator lens (Thorlabs 355392-C) and a cylindrical slow axis collimator lens (Thorlabs Lj1878L1-C). For $I_{DFB} = 400$ mA, $I_{mod} = 300$ mA and $I_{SOA} = 3$ A ($L_{SOA} = 2$ mm), based on the 2σ value of the Gaussian fits the near field diameter and the far field angle are respectively $242 \mu\text{m}$ and 4.4 mrad which leads to an M^2 value of 2.15 (slow axis).

V. CONCLUSION

We have designed a three-section bent MOPA which includes a DFB laser, a modulation section and a flared

SOA section. The MQW InGaAsP/InP structure have been optimized to maximize the output power and to reduce the vertical divergence. Thanks to the bent architecture of the device which reduces the facet reflections to the DFB laser, we have demonstrated a stable wavelength emission without mode-hopping for a DFB current ranging from the threshold to 500 mA. At high bias current, the SMSR is better than 45 dB. At 18°C the output power is superior to 400 mW. The far field exhibits a crescent-shaped and a FWHM divergence of $2.4 \times 23.5^\circ$. We have demonstrated that with an appropriate bias current, the modulation section allows signal attenuation with an extinction ratio of more than 35 dB with respect to the maximum transmittance. This section can be used to modulate the signal for data transmission.

REFERENCES

- [1] R. Menna *et al.*, "High power 1550 nm distributed feedback lasers with 440 mW CW output power for telecommunication applications," in *CLEO Tech. Dig.*, Baltimore, MD, USA, May 2001, pp. CPD12-1-CPD12-2.
- [2] W. Loh, F. J. O'Donnell, J. J. Plant, M. A. Brattain, L. J. Missaggia, and P. W. Juodawlkis, "Packaged, high-power, narrow-linewidth slab-coupled optical waveguide external cavity laser (SCOWECL)," *IEEE Photon. Technol. Lett.*, vol. 23, no. 14, pp. 974–976, Jul. 15, 2011.
- [3] M. L. Osowski *et al.*, "High-power semiconductor lasers at eye-safe wavelengths," *Proc. SPIE, Laser Technol. Defense Secur.*, vol. 7325, p. 73250V, May 2009.
- [4] M. Vilera, A. Pérez-Serrano, J. M. G. Tijero, and I. Esquivias, "Emission characteristics of a $1.5\text{-}\mu\text{m}$ all-semiconductor tapered master oscillator power amplifier," *IEEE Photon. J.*, vol. 7, no. 2, Apr. 2015, Art. ID 1500709.
- [5] M. Spreemann, M. Lichtner, M. Radziunas, U. Bandelow, and H. Wenzel, "Measurement and simulation of distributed-feedback tapered master-oscillator power amplifiers," *IEEE J. Quantum Electron.*, vol. 45, no. 6, pp. 609–616, Jun. 2009.
- [6] L. Hou, M. Haji, J. Akbar, and J. H. Marsh, "Narrow linewidth laterally coupled $1.55 \mu\text{m}$ AlGaInAs/InP distributed feedback lasers integrated with a curved tapered semiconductor optical amplifier," *Opt. Lett.*, vol. 37, no. 21, pp. 4525–4527, Nov. 2012.
- [7] X. Ai *et al.*, "Pseudo-random single photon counting for space-borne atmospheric sensing applications," in *Proc. IEEE Aerosp. Conf.*, Big Sky, MT, USA, Mar. 2014, pp. 1–10.
- [8] M. Faugeron *et al.*, "High-power, low RIN $1.55\text{-}\mu\text{m}$ directly modulated DFB lasers for analog signal transmission," *IEEE Photon. Technol. Lett.*, vol. 24, no. 2, pp. 116–118, Jan. 15, 2012.
- [9] M. Faugeron *et al.*, "High peak power, narrow RF linewidth asymmetrical cladding quantum-dash mode-locked lasers," *IEEE J. Sel. Topics Quantum Electron.*, vol. 19, no. 4, Jul./Aug. 2013, Art. ID 1101008.
- [10] M. Faugeron *et al.*, "High-power tunable dilute mode DFB laser with low RIN and narrow linewidth," *IEEE Photon. Technol. Lett.*, vol. 25, no. 1, pp. 7–10, Jan. 1, 2013.
- [11] C. E. Zah *et al.*, " $1.3 \mu\text{m}$ GaInAsP near-travelling-wave laser amplifiers made by combination of angled facets and antireflection coatings," *Electron. Lett.*, vol. 24, no. 20, pp. 1275–1276, Sep. 1988.
- [12] (Apr. 29, 2015). *BeamPROP Product Overview*. [Online]. Available: <http://optics.synopsys.com/rsoft/rsoft-passive-device-beamprop.html>
- [13] R. P. Ratowsky, S. Dijaili, J. Walker, F. Patterson, J. Kallman, and R. Deri, "Calculation of farfield distortion for a tilted-facet SOA," in *Opt. Soc. Amer. (OSA) Meeting Integr. Photon. Res.*, OSA Tech. Dig. Ser., vol. 6. 1996, paper PDP5.